

FAST-DECODING DIFFUSION LANGUAGE MODELS VIA PROGRESS-AWARE CONFIDENCE SCHEDULES

Amr Mohamed^{1,2*}, Yang Zhang², Michalis Vazirgiannis^{1,2}, Guokan Shang¹

¹MBZUAI, ²Ecole Polytechnique

ABSTRACT

Diffusion large language models (dLLMs) offer a promising alternative to autoregressive models, but their practical utility is severely hampered by slow, iterative sampling. We present *SchED*, a training-free, model-agnostic early-exit algorithm that aggregates full-span logit margins and halts decoding once a smooth, progress-dependent confidence threshold is met. We evaluated *SchED* on two dLLM families (*Dream* and *LLaDA*), in base and instruction-tuned variants across ten benchmarks spanning downstream tasks including multiple-choice question answering (MCQ), math, long-form QA/summarization, and translation. *SchED* delivers large, stable accelerations: on instruction-tuned models, it achieves $3.8\text{--}4.0\times$ speedups while retaining 99.8–100% of the baseline score on average. On base models, *SchED* yields consistent speedup gains with 99.1–100% performance retention, with up to $2.34\times$ under more aggressive settings. Using a conservative speed metric that heavily penalizes quality loss (QPS, $\gamma=4$), we show that *SchED* is robust and clearly outperforms prior confidence-based early-exit methods, which break down on long-form generation. An entropy analysis of the model’s token predictions reveals that instruction tuning speeds up the decay of predictive entropy. By turning genuine confidence stabilization into computational savings, *SchED* makes dLLM decoding substantially more efficient.

1 INTRODUCTION

Large Language Models (LLMs) have evolved rapidly in recent years, but the dominant decoding paradigm remains autoregressive (AR), which is inherently sequential and constrains opportunities for parallel generation and global context use (Brown et al., 2020; Yin et al., 2024; Zhang et al., 2025b). In response, Diffusion Large Language Models (dLLMs) have emerged as a credible alternative to AR decoding, offering compelling advantages such as parallel refinement, flexible infilling, and bidirectional attention over the partially generated sequence (Zou et al., 2023). This paradigm has matured rapidly, with efforts to train powerful base and instruct models from scratch (Ye et al., 2025), adapt existing AR checkpoints (Gong et al., 2024b; Nie et al., 2025), and push capabilities into complex domains like reasoning and planning, where they can outperform AR models on certain tasks (Phuong et al., 2025; Gong et al., 2024a). Recent systems demonstrate that dLLMs can be scaled and engineered with many of the same ingredients that power AR LLMs, including sparse mixture-of-experts (Huang et al., 2025), long-context extensions (Wang et al., 2025c), high-throughput inference pipelines for code generation (Song et al., 2025; Pal et al., 2025), and principled scaling analyses for masked diffusion objectives (Li et al., 2024). Collectively, these results position dLLMs as a practical family of foundation-model architectures with distinct decoding affordances.

Despite this promise, decoding efficiency remains a central bottleneck for dLLMs. dLLM generation proceeds via a reverse-diffusion chain with many refinement steps. In addition, practitioners must choose step budgets and transfer schedules *a priori*, often conservatively, to avoid quality loss. This leads to unnecessary computation on “easy” inputs and, when heuristic decoding parameter choices (e.g., step budgets) are too extreme, unstable behavior across tasks. A growing body of work addresses this bottleneck through training-free early-commit methods, which exploit

*Correspondence: amr.mohamed@mbzuai.ac.ae

the empirical observation that predictions often stabilize well before the final diffusion step (Pengxiang et al., 2025). Dynamic policies modulate exploration versus acceleration across the chain, using signals like historical logits or local determinism to reduce redundant steps (Wei et al., 2025; Wang et al., 2025b; Or-El et al., 2025). Other lines of work focus on error correction and refinement, enabling models to revise their own outputs by re-masking low-confidence tokens (Zhang et al., 2025a; Su et al., 2025). Few- and one-step routes also address this bottleneck by transferring ideas from continuous diffusion via curriculum, consistency distillation, or flow matching (Sahoo et al., 2025; Chen et al., 2025; Meister et al., 2024). Orthogonal efforts reduce per-step latency with caching adapted to bidirectional refinement (Yuan et al., 2025b; Wang et al., 2025a) and with speculative mechanisms that draft and verify tokens in parallel (Sohoni et al., 2025; Yuan et al., 2025a). While impactful, these approaches often require additional training, introduce auxiliary models, or rely on complex heuristics, leaving room for a simple, training-free, and *architecture-agnostic* early-exit principle.

We revisit diffusion decoding as a *when-to-stop* problem and introduce *SchED*, a *schedule-based* early-exit mechanism that is both training-free and model-agnostic. Concretely, we aggregate token-level confidence (top-2 logit margins) over an answer region and compare it against a *monotonic, continuous* threshold that relaxes smoothly with normalized diffusion progress. By decoupling the confidence target from step count and making the threshold a smooth function of progress, the sampler exits *as soon as* predictions are stable, while avoiding the brittleness of hard phase changes or fixed budgets. *SchED* composes with standard transfer schedules (single-suffix or block diffusion) and requires no changes to model training (Nie et al., 2025; Ye et al., 2025).

We evaluate *SchED* across two diffusion LLM families (a single-block Dream decoder and a block-diffusion LLaDA decoder), each in base and instruction-tuned variants, on ten diverse benchmarks covering multiple-choice, math, long-form QA/summarization, and translation. On instruction-tuned models, *SchED* retains 99.8–100% of baseline quality on average while yielding 3.8–4.0× speedups and outperforming recent training-free early-commit methods on a conservative quality-penalized speed metric; on base models, it delivers smaller but consistent gains at near-parity quality (§5). Together, these results show that *SchED* can substantially reduce diffusion decoding costs without sacrificing quality, and that instruction tuning lowers the confidence barrier for early exit in QA-style tasks, making it particularly effective in that regime. This paper makes the following contributions:

1. **Training-free, schedule-based early exit.** We introduce *SchED* (**S**chedule-based **E**arly **D**ecoding) for diffusion language models, which thresholds a full-span logit-margin aggregate against a smooth, progress-dependent schedule (linear, cosine, exponential), enabling stable, architecture-agnostic stopping without retraining.
2. **Strong efficiency at near-parity quality.** On instruction-tuned models, *SchED* retains 99.8–100% of baseline performance while achieving 3.8–4× speedups. On base models, it delivers 99.1–100% of baseline accuracy with 1.04–1.14× speedups in conservative settings, and up to 2.34× under more extreme schedules.
3. **Principled quality-speed trade-off metric.** We propose *Quality–Penalized Speed (QPS)* (Eq. 14), which conservatively penalizes accuracy drops. With $\gamma=4$, SCED schedules achieve QPS values of 1.01–2.03 on Dream Base and 3.24–4.30 on Dream Instruct, outperforming prior early-commit methods (Table 3).
4. **Mechanistic explanation via entropy-based analysis.** Analyzing predictive-entropy trajectories over the answer span shows that instruction tuning accelerates confidence stabilization, aligning with progress-aware thresholds and explaining early exits without quality loss (Fig. 1).

SchED builds on the vanilla dLLM denoising process by enforcing a smooth, progress-dependent confidence threshold over the generated span, exploiting the bidirectional, parallel strengths of dLLMs to achieve end-to-end efficiency without retraining (Zou et al., 2023; Nie et al., 2025; Ye et al., 2025; Gong et al., 2024a). Code is publicly available¹.

¹<https://github.com/amr-mohammed/SchED.git>

2 RELATED WORK

Diffusion LLMs. Recent work establishes diffusion language models (dLLMs) as a viable alternative to autoregressive (AR) models, training either from scratch or by adapting AR checkpoints. LLaDA trains a bidirectional Transformer with a forward masking process and a reverse denoising chain, demonstrating strong pretraining and SFT performance (Nie et al., 2025). Several lines adapt AR models into diffusion ones for fair, scalable comparisons across sizes and tasks (Gong et al., 2024b), while Dream-7B advances recipe and refinement design and releases base/instruct variants (Ye et al., 2025). Architectural advancements have also been integrated, with models like LLaDA-MoE demonstrating the successful application of sparse Mixture-of-Experts to dLLMs, achieving competitive performance with significantly reduced active parameters (Huang et al., 2025). The capabilities of dLLMs are also expanding to long-context scenarios; The work like UltraLLaDA shows that techniques such as Rotary Positional Embedding (RoPE) scaling can be adapted to extend context windows to 128K tokens (Wang et al., 2025c). Seed Diffusion emphasizes high-throughput inference for code models (Song et al., 2025). Moreover, formal studies on the scaling laws of masked diffusion models have further established their viability, demonstrating a scaling rate comparable to autoregressive models (Li et al., 2024). Survey and perspective papers summarize the landscape, strengths (parallelism, infilling, global context), and open questions (Zou et al., 2023).

Sampling efficiency and early commit. A central bottleneck for dLLMs is the number of refinement steps. Prophet exploits the empirical observation that answers often stabilize well before the final step and proposes a training-free early-commit rule based on top-2 logit gaps (Pengxiang et al., 2025). Complementary dynamic policies include SlowFast Sampling, which alternates exploratory vs. accelerated phases guided by certainty/convergence/position principles and can combine with caching (Wei et al., 2025); Duo transfers continuous-diffusion techniques (curriculum learning, consistency distillation) to discrete diffusion to enable few-step sampling (Sahoo et al., 2025); and DLM-One studies one-step generation via score distillation in continuous spaces (Chen et al., 2025). Orthogonal to reducing step counts, other efforts focus on reducing per-step latency by developing novel caching mechanisms like dKV-Cache and d²Cache, which adapt key-value caching to the bidirectional nature of dLLMs (Yuan et al., 2025b; Wang et al., 2025a). Furthermore, speculative decoding has been adapted for the diffusion framework, using the model’s own predictions to draft and verify multiple tokens in parallel, as seen in Spiffy and Self Speculative Decoding (Sohoni et al., 2025; Yuan et al., 2025a). Our work also treats decoding as a *when-to-stop* problem, but (unlike Prophet) we introduce a smooth confidence *schedule* that relaxes thresholds over progress, yielding stable, training-free early exit that is *agnostic to architecture and training*.

3 METHODS

In this section, we formalize discrete diffusion language models and introduce *SchED*, our schedule-based early decoding mechanism. We first review the forward and reverse masking processes and the standard training objective, then describe our confidence aggregation scheme, progress-dependent threshold schedules, and the resulting early-exit decoding algorithm.

3.1 PRELIMINARIES: DISCRETE DIFFUSION LANGUAGE MODELS

Setup and notation. Let \mathcal{V} denote the vocabulary and $[mask]$ a special placeholder token. Given a prompt prefix, generation proceeds over T reverse-diffusion steps $t \in \{1, \dots, T\}$ on sequences $x_t \in (\mathcal{V} \cup \{[mask]\})^L$. At each step, given the current noised sequence x_t and prompt x_{prompt} , the model produces logits

$$L_t = f_\theta(x_{\text{prompt}}, x_t, t) \in \mathbb{R}^{L \times |\mathcal{V}|}, \quad (1)$$

and per-position categorical distributions

$$p_{t,i}(\cdot | x_{\text{prompt}}, x_t) = \text{softmax}(L_{t,i}) \in \Delta^{|\mathcal{V}|}. \quad (2)$$

We write $A \subseteq \{1, \dots, L\}$ for the answer region used later for confidence aggregation, and define normalized diffusion progress $p = t/T$.

Forward (masking) process q . We model discrete diffusion as a progressive *masking process* that corrupts a clean sequence $x_0 \in \mathcal{V}^L$ over T steps. Let $\beta_t \in [0, 1)$ be a step-dependent masking rate and define the per-step transition

$$q(x_t | x_{t-1}) = \prod_{i=1}^L [(1 - \beta_t) \delta(x_{t,i} = x_{t-1,i}) + \beta_t \delta(x_{t,i} = [\text{mask}])]. \quad (3)$$

Writing $\bar{\alpha}_t = \prod_{s=1}^t (1 - \beta_s)$ for the token survival probability after t steps, the t -step marginal becomes

$$q(x_t | x_0, t) = \prod_{i=1}^L [\bar{\alpha}_t \delta(x_{t,i} = x_{0,i}) + (1 - \bar{\alpha}_t) \delta(x_{t,i} = [\text{mask}])]. \quad (4)$$

Reverse (denoising) process p_θ . Diffusion language models define a learned reverse chain that progressively *unmasks* tokens from x_T (fully masked) to x_0 (fully decoded) by factoring over individual positions:

$$p_\theta(x_{t-1} | x_{\text{prompt}}, x_t) = \prod_{i=1}^L p_\theta(x_{t-1,i} | x_{\text{prompt}}, x_t). \quad (5)$$

Each per-position term is then parameterized as a categorical distribution based on the model’s current output:

$$p_\theta(x_{t-1,i} | x_{\text{prompt}}, x_t) = \text{Cat}(x_{t-1,i}; p_{t,i}(\cdot | x_{\text{prompt}}, x_t)), \quad (6)$$

where $p_{t,i}(\cdot | x_{\text{prompt}}, x_t)$ denotes the model’s categorical prediction at position i given the partially masked sequence x_t and prompt context x_{prompt} at timestep t .

Masked diffusion with partial unmasking (transfer schedule). To control generation granularity, only a subset of masked positions are updated at each step. Let $M_t = \{i : x_{t,i} = [\text{mask}]\}$ and let $\pi_t(i) \in \{0, 1\}$ indicate whether position i is selected for update under a *transfer schedule*. Given the model’s predictive distribution $p_{t,i}(\cdot | x_{\text{prompt}}, x_t)$ at timestep t , the step operator is

$$x_{t-1,i} = \begin{cases} x_{t,i}, & \text{if } i \notin M_t \text{ or } \pi_t(i) = 0, \\ \hat{x}_{t,i}, & \text{if } i \in M_t \text{ and } \pi_t(i) = 1, \end{cases} \quad (7)$$

where $\hat{x}_{t,i}$ is obtained either deterministically or stochastically,

$$\hat{x}_{t,i} = \arg \max_v p_{t,i}(v | x_{\text{prompt}}, x_t) \quad \text{or} \quad \hat{x}_{t,i} \sim \text{Cat}(p_{t,i}(\cdot | x_{\text{prompt}}, x_t)).$$

Block-diffusion variants (e.g., LLaDA) choose π_t over contiguous token blocks, whereas single-block variants (e.g., Dream) often select the entire suffix or a fixed proportion. $\sim \text{Cat}(p_{t,i}(\cdot | x_{\text{prompt}}, x_t))$.

Training objective. Diffusion language models are typically trained to invert the forward masking process via a masked-token objective over uniformly sampled timesteps:

$$\mathcal{L}(\theta) = \mathbb{E}_{x_0 \sim \mathcal{D}} \mathbb{E}_{t \sim \mathcal{U}\{1:T\}} \mathbb{E}_{x_t \sim q(\cdot | x_0, t)} \left[- \sum_{i \in M_t} \log p_{t,i}(x_{0,i} | x_{\text{prompt}}, x_t) \right]. \quad (8)$$

Here x_t is obtained by applying the forward kernel at timestep t , and $p_{t,i}(x_{0,i} | x_{\text{prompt}}, x_t)$ is shorthand for the model’s predictive probability $p_\theta(x_{0,i} | x_{\text{prompt}}, x_t, t)$ at position i given the partially noised context. This formulation encourages the model to predict the original tokens at masked sites given partially noised contexts, aligning p_θ with the forward corruption kernel q .

3.2 SchED: SCHEDULE-BASED EARLY DECODING

We propose *SchED*, a confidence- and progress-aware early-exit algorithm for diffusion decoding. At each step, *SchED* thresholds the model’s aggregated token confidence against a smooth, nonincreasing function of progress p , i.e., $(\bar{g}_t \geq \tau(p))$. This design builds on the assumption that per-token confidence typically rises as denoising proceeds, allowing generation to terminate precisely

when predictions stabilize rather than at a fixed budget. The complete, model-agnostic procedure is summarized in Algorithm 1.

Algorithm 1 SchED: Schedule-Based Early Decoding for Diffusion Language Models

Require: model M ; prompt tokens x_{prompt} ; generation length L_{gen} ; max steps T ;

- 1: answer region $A \subseteq \{1, \dots, L\}$; aggregator Agg ;
- 2: threshold schedule $\tau(p; \tau_{\text{high}}, \tau_{\text{low}})$;
- 3: transfer schedule π_t (or block policy for block diffusion).

Ensure: completed sequence x

- 4: Initialize $x \leftarrow [x_{\text{prompt}}; [\text{mask}] \times L_{\text{gen}}]$
- 5: **for** $t = 1$ to T **do**
- 6: $L_t \leftarrow M(x)$ ▷ Model logits at step t
- 7: Compute token-level margins $g_{t,i} = L_{t,i}^{(1)} - L_{t,i}^{(2)}$ for $i \in A$
- 8: Aggregate confidence $\bar{g}_t \leftarrow \text{Agg}(\{g_{t,i} : i \in A\})$
- 9: $p \leftarrow t/T$ ▷ Normalized diffusion progress
- 10: **if** $\bar{g}_t \geq \tau(p; \tau_{\text{high}}, \tau_{\text{low}})$ **then**
- 11: Fill all remaining $[\text{mask}]$ tokens with current argmax predictions and **return** x
- 12: **end if**
- 13: Identify masked positions $M_t = \{i : x_i = [\text{mask}]\}$
- 14: Select positions $S_t \leftarrow \{i \in M_t : \pi_t(i) = 1\}$
- 15: Set $x_{S_t} \leftarrow \arg \max_v L_{t,S_t,v}$
- 16: **end for**
- 17: **return** x ▷ If no early exit occurred within T steps

SchED tracks how model confidence evolves throughout denoising and terminates the process once confidence exceeds a progress-dependent threshold, preventing redundant refinement after predictions have stabilized.

Confidence measurement. Following the work of Pengxiang et al. (2025), we quantify model confidence using token-level logit margins, which capture how decisively the model prefers its top prediction over alternatives. A region-level confidence score is obtained by aggregating top-2 margins over the *entire answer region* A (i.e., the full model response span):

$$\bar{g}_t = \text{Agg}(\{g_{t,i} : i \in A\}), \quad \text{with } \text{Agg} = \text{mean by default}, \quad (9)$$

so that $\bar{g}_t = 1/|A| \sum_{i \in A} g_{t,i}$ in our experiments. Importantly, $g_{t,i}$ uses the *current* logits at step t for every $i \in A$. All thresholds ($\tau_{\text{high}}, \tau_{\text{low}}$) are expressed in *logit units*.

Early-exit trigger. An early exit is triggered when the aggregated confidence surpasses a smooth, progress-dependent threshold schedule $\tau(p)$:

$$\bar{g}_t \geq \tau(p), \quad (10)$$

where $\tau : [0, 1] \rightarrow \mathbb{R}_{\geq 0}$ is a nonincreasing function of the generation progress $p = t/T$. This formulation ensures that the confidence requirement for stopping is highest at the beginning of generation and gradually relaxes as denoising proceeds, allowing the model to terminate decoding once its predictions have stabilized.

Smooth threshold schedules. The threshold function $\tau(p)$ controls when the sampler terminates. We parameterize τ using a pair $(\tau_{\text{high}}, \tau_{\text{low}})$, which specify the initial and final confidence thresholds, and an optional slope parameter $k > 0$. We explore three families of schedules:

$$\text{Linear: } \tau_{\text{lin}}(p) = \tau_{\text{high}} + (\tau_{\text{low}} - \tau_{\text{high}})p, \quad (11)$$

$$\text{Cosine: } \tau_{\text{cos}}(p) = \tau_{\text{low}} + \frac{1}{2}(\tau_{\text{high}} - \tau_{\text{low}})(1 + \cos(\pi p)), \quad (12)$$

$$\text{Exponential: } \tau_{\text{exp}}(p) = \tau_{\text{low}} + (\tau_{\text{high}} - \tau_{\text{low}})e^{-kp}, \text{ with } k > 0. \quad (13)$$

Each schedule defines a smooth, nonincreasing trajectory from τ_{high} at $p = 0$ to τ_{low} at $p = 1$, offering different degrees of early-exit aggressiveness and stability control while avoiding the brittleness of fixed thresholds or discrete rules.

4 EXPERIMENTAL SETTINGS

We evaluate *SchED* across a diverse suite of multiple-choice and long-form generation tasks, assessing its ability to accelerate diffusion decoding while preserving output quality. Specifically, we compare its denoising efficiency against two baselines: (i) standard diffusion sampling without early exit and (ii) Prophet (Pengxiang et al., 2025). Unless otherwise stated, we fix the upper threshold at ($\tau_{\text{high}} = 7.5$) and, for each schedule family, evaluate two lower-threshold settings: a relaxed ($\tau_{\text{low}} = 0$) and a more conservative ($\tau_{\text{low}} = 2.5$), yielding a smooth, monotonic relaxation over diffusion progress in both regimes.

Models. *SchED* is model-agnostic and can be applied to any dLLM without architectural or training modifications. To demonstrate its generality, we evaluate on two representative dLLM families that employ distinct decoding paradigms: the *Dream* family (Ye et al., 2025), which performs full-sequence refinement using a single-block decoder, and the *LLaDA* family (Nie et al., 2025), which adopts a block-diffusion strategy that denoises contiguous token segments. Each family is evaluated in both base and instruction-tuned variants, and we apply the low-confidence remasking strategy across all models.

Benchmarks. We evaluate on GPQA (Rein et al., 2023), GSM8K (Cobbe et al., 2021), HellaSwag (Zellers et al., 2019), MMLU (Hendrycks et al., 2020), PIQA (Bisk et al., 2020), and Winogrande (Sakaguchi et al., 2020). For long-context evaluation, we use tasks from the Long-Bench suite (Bai et al., 2023), specifically LongBench–HotpotQA (Yang et al., 2018) and Long-Bench–MultiNews (Fabbri et al., 2019). For translation, we use WMT14 En–Fr (Bojar et al., 2014) (5-shot) and WMT16 En–De (Bojar et al., 2016) (5-shot). Each benchmark includes runs for the baseline, Prophet, and the full set of linear, cosine, and exponential schedules across both model variants.

Evaluation metrics and framework. For **multiple-choice** (MCQ) benchmarks, *GPQA*, *HellaSwag*, *MMLU*, *PIQA*, and *Winogrande*, we report **accuracy**. For *GSM8K* we also report **accuracy** based on the generated final answer. For HotpotQA, we report token-level **F1-score**; for Multi-News, we report **ROUGE** (Lin, 2004); and for translation (*WMT14 En–Fr*, *WMT16 En–De*), we report **CHRF**. All evaluations are conducted using the *Language Model Evaluation Harness* (Gao et al., 2024).

Efficiency metric for quality–speed trade-offs. Reporting quality and speedup separately can obscure Pareto differences between methods. To jointly capture both aspects, we define the *Quality-Penalized Speed* (QPS) metric:

$$\text{QPS}_\gamma = \text{speedup} \times \left(\frac{\text{score}}{\text{baseline score}} \right)^\gamma, \quad (14)$$

where the exponent $\gamma \geq 1$ controls how strongly quality degradation is penalized. Higher values of γ emphasize fidelity over raw acceleration; in our experiments, we use $\gamma=4$ to provide conservative and interpretable efficiency comparisons.

5 RESULTS

Method	GPQA	HellaSwag	MMLU	PIQA	Winogrande	GSM8K	HotpotQA	MultiNews	WMT14 En–Fr	WMT16 En–De	Average
Baseline	28.57 (×1.00)	79.15 (×1.00)	73.39 (×1.00)	88.68 (×1.00)	75.61 (×1.00)	77.10 (×1.00)	8.67 (×1.00)	21.24 (×1.00)	52.99 (×1.00)	47.70 (×1.00)	55.31 (×1.00)
Prophet	28.79 (×1.13)	79.15 (×1.00)	73.37 (×1.03)	88.68 (×1.20)	75.61 (×1.00)	77.03 (×1.07)	8.68 (×1.03)	21.21 (×1.06)	52.99 (×1.11)	47.57 (×1.06)	55.31 (×1.07)
Cosine (7.5, 0)	28.12 (×1.23)	79.15 (×1.02)	73.40 (×1.09)	88.57 (×1.22)	75.61 (×1.01)	76.98 (×1.02)	8.74 (×1.12)	21.28 (×1.13)	52.79 (×1.23)	45.64 (×1.20)	55.02 (×1.14)
Cosine (7.5, 2.5)	28.79 (×1.11)	79.15 (×1.00)	73.37 (×1.02)	88.68 (×1.14)	75.61 (×1.00)	77.03 (×1.07)	8.68 (×1.02)	21.21 (×1.05)	52.99 (×1.10)	47.64 (×1.05)	55.31 (×1.06)
Linear (7.5, 0)	29.02 (×1.19)	79.15 (×1.00)	73.40 (×1.06)	88.57 (×1.22)	75.61 (×1.00)	76.95 (×1.13)	8.66 (×1.08)	21.26 (×1.10)	52.87 (×1.18)	46.43 (×1.15)	55.19 (×1.11)
Linear (7.5, 2.5)	28.79 (×1.10)	79.15 (×1.00)	73.37 (×1.02)	88.68 (×1.03)	75.61 (×1.00)	77.03 (×1.06)	8.67 (×1.02)	21.21 (×1.05)	53.00 (×1.09)	47.67 (×1.04)	55.32 (×1.04)
Exp-k=2 (7.5, 0)	24.33 (×1.19)	79.13 (×1.00)	73.50 (×1.07)	88.47 (×1.27)	75.77 (×1.00)	77.63 (×1.11)	8.17 (×1.07)	20.94 (×1.10)	53.16 (×1.18)	46.81 (×1.13)	54.79 (×1.11)
Exp-k=2 (7.5, 2.5)	24.33 (×1.10)	79.13 (×1.00)	73.49 (×1.02)	88.63 (×1.06)	75.77 (×1.00)	77.71 (×1.06)	8.16 (×1.03)	20.88 (×1.05)	53.26 (×1.09)	47.60 (×1.04)	54.90 (×1.04)
Exp-k=16 (7.5, 0)	24.78 (×2.04)	77.14 (×2.50)	73.05 (×2.50)	87.92 (×2.50)	72.85 (×2.50)	62.77 (×3.05)	15.75 (×2.78)	21.74 (×2.75)	52.87 (×1.44)	44.75 (×1.39)	53.36 (×2.34)
Exp-k=16 (7.5, 2.5)	23.88 (×1.14)	79.13 (×1.00)	73.53 (×1.18)	88.47 (×1.36)	75.77 (×1.00)	77.63 (×1.08)	8.22 (×1.07)	20.92 (×1.07)	53.26 (×1.13)	47.51 (×1.07)	54.83 (×1.11)

Table 1: *Dream Base*: benchmark scores with speedups (×). Two thresholds—conservative (7.5, 2.5) and relaxed (7.5, 0). Column best in **bold**, second-best in *italic*.

Tables 1 and 2 report results for Dream Base and Dream Instruct, respectively.

Method	GPAQ	HellaSwag	MMLU	PIQA	Winograde	GSM8K	HotpotQA	MultiNews	WMT14 En-Fr	WMT16 En-De	Average
Baseline	30.36 (×1.00)	79.91 (×1.00)	80.69 (×1.00)	73.02 (×1.00)	85.80 (×1.00)	74.66 (×1.00)	27.51 (×1.00)	24.39 (×1.00)	55.82 (×1.00)	49.85 (×1.00)	58.20 (×1.00)
Prophet	28.79 (×16.45)	26.69 (×7.81)	78.73 (×1.14)	72.33 (×1.01)	72.58 (×1.03)	66.54 (×1.02)	27.87 (×4.51)	2.77 (×31.21)	20.17 (×23.93)	15.28 (×27.87)	41.18 (×11.60)
Cosine (7.5, 0)	30.58 (×15.96)	78.54 (×2.11)	80.81 (×1.56)	73.06 (×1.14)	85.96 (×1.32)	74.11 (×1.61)	27.46 (×3.24)	24.39 (×6.60)	55.82 (×2.39)	49.86 (×2.81)	58.06 (×3.87)
Cosine (7.5, 2.5)	30.58 (×15.93)	79.53 (×2.08)	80.75 (×1.43)	73.08 (×1.11)	85.91 (×1.23)	74.27 (×1.28)	27.47 (×3.14)	24.38 (×6.59)	55.82 (×2.34)	49.85 (×2.77)	58.16 (×3.79)
Linear (7.5, 0)	30.58 (×16.08)	79.00 (×2.11)	80.81 (×1.56)	73.14 (×1.14)	85.96 (×1.32)	74.11 (×1.49)	27.48 (×3.26)	24.39 (×3.02)	55.82 (×2.38)	49.86 (×2.80)	58.11 (×3.89)
Linear (7.5, 2.5)	30.58 (×16.01)	79.76 (×2.08)	80.76 (×1.43)	73.09 (×1.10)	85.83 (×1.22)	74.27 (×1.27)	27.47 (×3.17)	24.38 (×6.59)	55.82 (×2.33)	49.85 (×2.76)	58.16 (×3.79)
Exp- $k=2$ (7.5, 0)	30.58 (×16.32)	79.45 (×2.14)	80.77 (×1.62)	73.11 (×1.21)	86.16 (×1.54)	74.35 (×1.67)	26.71 (×3.47)	24.56 (×6.66)	55.76 (×2.40)	49.84 (×2.76)	58.14 (×3.97)
Exp- $k=2$ (7.5, 2.5)	30.13 (×16.18)	80.21 (×2.10)	80.69 (×1.54)	73.25 (×1.11)	86.24 (×1.23)	74.51 (×1.53)	26.91 (×3.23)	24.60 (×6.57)	55.76 (×2.33)	49.84 (×2.71)	58.21 (×3.85)
Exp- $k=16$ (7.5, 0)	29.46 (×18.64)	32.98 (×3.73)	79.31 (×5.00)	58.81 (×2.50)	84.55 (×5.00)	73.80 (×5.00)	26.20 (×5.79)	23.99 (×17.38)	53.53 (×5.56)	49.72 (×3.17)	51.12 (×5.44)
Exp- $k=16$ (7.5, 2.5)	30.58 (×17.16)	79.68 (×2.13)	79.31 (×2.50)	72.78 (×1.55)	84.49 (×2.29)	72.61 (×2.10)	26.58 (×4.33)	24.26 (×7.21)	55.76 (×2.38)	49.84 (×2.74)	57.59 (×4.48)

Table 2: *Dream Instruct*: benchmark scores with speedups (×). Two thresholds—conservative (7.5, 2.5) and relaxed (7.5, 0). Column best in **bold**, second-best in *italic*.

Dream Base. With conservative smooth schedules ($\tau_{\text{high}}, \tau_{\text{low}} = (7.5, 2.5)$), linear, cosine, and exp- $k=2$, we observe steady 1.04–1.14× average speedups at near-parity quality, with marginal task gains (e.g., *WMT14 En-Fr*: $\Delta+0.27$) under exp- $k=2$ (7.5, 2.5). Fast-decaying exponentials (large k) with $\tau_{\text{low}} = 2.5$ remain close to parity, but do not increase the mean speed beyond $\approx 1.1\times$; setting $\tau_{\text{low}} = 0$ yields 2.34× average speed (exp- $k=16$), with task-specific gains that are most pronounced on *HotpotQA* ($\Delta+7.1$); however, at an overall quality cost of $\approx 2\%$. Prophet offers $\approx 1.07\times$ average speed with near-parity accuracy, providing limited practical benefits relative to smooth schedules.

Dream Instruct. Under the same conservative thresholds, smooth schedules deliver ≈ 3.8 –4.0× average speedups at near parity: table averages cluster around the baseline (e.g., 58.06–58.22 vs. 58.20). Notably, the large- k (fast-decaying) exponential with (7.5, 2.5) attains 4.48×, while remaining close to parity (57.59, $\Delta-1\%$). Less conservative settings with $\tau_{\text{low}} = 0$ also preserve translation near baseline with 2.3–2.8× speed (e.g., cosine and linear). For the large- k exponential, ($k=16$, $\tau_{\text{low}}=0$) delivers the most pronounced speedups while remaining near parity on most benchmarks; however, it exhibits large degradations on *HellaSwag* and *PIQA*.

LLaDA exhibits similar trends to those observed on Dream: conservative schedules provide reliable speedups at near-parity quality on the base model; the instruction-tuned variant yields higher speedups. Fast-decaying settings risk over-commitment that degrades math and long-form. While Prophet provides high speedups, it underperforms on long-form generation. Detailed LLaDA Base and Instruct results are in Tables 7 and 8; additional schedule ablations for Dream and LLaDA appear in Appendix B.

Efficiency results. Table 3 reports *Quality-Penalized Speed* (QPS; $\gamma=4$). On *Dream Base*, smooth schedules concentrate in the ≈ 1.01 –1.12 range, reflecting the near-parity averages in Table 1 (e.g., 55.02–55.32 vs. baseline 55.31) coupled with modest mean speedups (≈ 1.04 –1.14×). The highest base-model efficiency is achieved by the rapidly decaying exponential, Exp- $k=16$, (7.5, 0), with **2.03**, driven by a large average speedup (2.34×), and average-score drop of -1.95 . Prophet attains 1.07, consistent with its near-baseline averages and limited acceleration.

On *Dream Instruct*, QPS values increase substantially in line with the larger mean speedups observed in Table 2 (≈ 3.8 –4.0× for conservative smooth schedules) while maintaining average scores close to baseline. The best overall result, **4.30**, is obtained by Exp- $k=16$, (7.5, 2.5), which combines a near-parity average score (57.59) with a pronounced 4.48× mean speedup. Other smooth schedules lie tightly in the 3.78–3.95 band. Prophet trails at 2.91, reflecting weaker average scores and failures on long-form despite notable raw speed. Overall, *SchED* consistently yields higher QPS₄ than Prophet; the top settings pair near-parity average performance with substantial step reductions, which explains their leading efficiency.

Method	Dream Base	Dream Instruct
Cosine (7.5, 0)	1.12	3.83
Cosine (7.5, 2.5)	1.06	3.78
Linear (7.5, 0)	1.10	3.87
Linear (7.5, 2.5)	1.04	3.78
Exp- $k=2$ (7.5, 0)	1.07	3.95
Exp- $k=2$ (7.5, 2.5)	1.01	3.85
Exp- $k=16$ (7.5, 0)	2.03 ↑	3.24
Exp- $k=16$ (7.5, 2.5)	1.07	4.30 ↑
Prophet	1.07	2.91

Table 3: **QPS** ($\gamma=4$) for all *SchED* variants and Prophet. ↑ Higher is better.

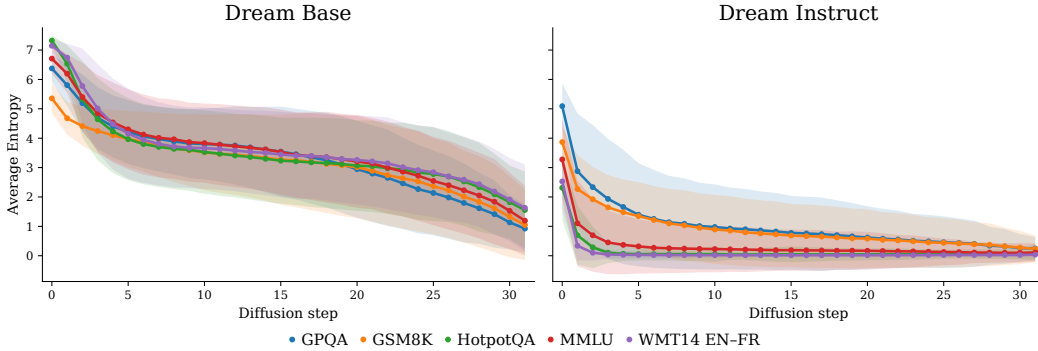


Figure 1: Mean predictive entropy across diffusion steps for five input types (*GPQA*, *GSM8K*, *HotpotQA*, *MMLU*, *WMT14 EN*→*FR*). Curves show per-token entropy (*nats/token*) averaged over evaluation samples; shaded bands denote one standard deviation across samples. Both Dream Base and Dream Instruct exhibit monotonically decreasing entropy as denoising progresses.

6 ANALYSIS

To better understand the differences in speedup values between *base* and *instruct* models, and the variation in speedups across benchmarks, we analyze how predictive uncertainty evolves over the reverse-diffusion chain. We track per-token predictive entropy on the generated region at each step t . Using the per-position distributions $p_{t,i}$ state x_t , the mean per-token entropy is

$$\bar{H}_t = \frac{1}{|S|} \sum_{i \in S} \left(- \sum_{v \in \mathcal{V}} p_{t,i}(v|x_{\text{prompt}}, x_t) \log p_{t,i}(v|x_{\text{prompt}}, x_t) \right). \quad (15)$$

where $p_{t,i}(v)$ denotes the model’s step- t predictive distribution at position i , computed from logits $L_{t,i}$ given x_{prompt} and x_t (Eq. 6).

Results are presented in Figure 1. *Dream Instruct* starts the denoising phase with higher entropy on math-heavy prompts (*GPQA* and *GSM8K*) and decays more slowly in the earliest steps than on *MMLU*, *HotpotQA*, and *WMT14*, yet the trajectories converge to similarly low final entropies. Notably, the instruct curves show a rapid early drop followed by nearly uniform per-step decreases, a stepwise profile consistent with Dream’s masked diffusion decoding, where at each reverse-diffusion step the model updates high-confidence tokens in parallel and thereby reduces uncertainty in approximately regular increments across the chain. CART’s context-adaptive token-level noise rescheduling further sharpens this behavior by encouraging more confident predictions at positions with stronger local context, particularly near the prompt. By contrast, *Dream Base* shows more overlapping trajectories across benchmarks and higher residual entropy overall, suggesting less decisive posteriors for QA-style inputs. This aligns with the smaller speedups obtained by schedule-based early exit on Base models (Tables 1–2).

7 DISCUSSION

The findings reported in Section 5 and Section 6 demonstrate that a progress-aware scheduling strategy effectively translates model confidence into computational savings, with an unusually high degree of robustness across tasks and model families. For instruction-tuned variants, *Sched* attains speedups of up to approximately 17×, while preserving full baseline accuracy and achieves average accelerations of up to about 4×, with overall accuracies essentially indistinguishable from the baseline, whereas base models exhibit more moderate yet consistently positive improvements. The entropy patterns in Figure 1 elucidate this discrepancy. Instruction tuning steers the model toward confident, QA-oriented completions, leading to a rapid reduction in uncertainty over the answer span. For *Dream Instruct*, this reduction follows a characteristic profile: an initial, pronounced decline, followed by approximately uniform stepwise decreases. By contrast, *Dream Base* retains higher entropy with flatter and more overlapping trajectories across benchmarks, postponing the

point at which aggregated confidence exceeds the stopping criterion and thereby constraining the attainable speedups.

The stopping criterion is central to the method’s stability. *SchED* compares a sequence-level logit–margin aggregate to a smooth, nonincreasing function of normalized diffusion progress $p = t/T$, imposing a stringent requirement at early steps and gradually relaxing it thereafter. This construction links the decision to terminate directly to the evolution of model certainty, dampens transient spikes, and triggers exit when predictions have effectively converged rather than at a pre-determined step count; using the entire generated span for aggregation further stabilizes the decision relative to short-prefix estimates, at the expense of modest additional computation. Empirically, conservative cosine and linear schedules maintain performance very close to the baseline while substantially reducing the number of refinement steps, and the QPS metric with $\gamma = 4$ indicates that these smooth schedules consistently achieve high quality–efficiency trade-offs. In contrast, rapidly decaying exponential schedules (large k , $\tau_{\text{low}} = 0$) yield greater acceleration but incur noticeable accuracy losses. Prophet’s degradation on long-form generation arises from computing confidence over a fixed, localized region and employing a discrete commit rule, which allows localized confidence spikes to induce premature termination while later portions of the output remain under-resolved, leading to reduced ROUGE and F1. *SchED* mitigates these issues by aggregating over the full generated sequence, making the threshold explicitly progress-dependent, and avoiding auxiliary suffix prompts that could artificially inflate early certainty.

Across tasks, the behavior of the stopping criterion is strongly input dependent. Math-oriented benchmarks exhibit distinct profiles: *GPQA*, although mathematically challenging, is multiple choice, so the presence of explicit answer options enables the model to reach relatively high confidence earlier in the diffusion process, even at nontrivial difficulty. By contrast, *GSM8K* also involves mathematical reasoning but requires free-form solutions; here confidence must build over a longer span, and the entropy trajectories indicate that additional refinement steps are needed before the schedule’s threshold is reliably exceeded. Long-form generation tasks benefit most from smoothing and full-span aggregation, since evaluation quality depends on maintaining coherent, accurate content throughout the response rather than producing an early, locally confident fragment. Translation occupies an intermediate regime: schedules keep CHRF close to baseline while still reducing the number of steps, reflecting the combination of bidirectional refinement and comparatively tight lexical and semantic constraints on the target.

These regularities are not specific to a single model family: LLaDA exhibits analogous behavior, with conservative smooth schedules improving efficiency at near-parity quality on base variants and yielding substantially larger gains on instruction-tuned models. In aggregate, progress-aware thresholds provide consistent acceleration, and the choice of schedule should be aligned with the tolerated error budget. Conservative configurations are appropriate when preserving fidelity is critical, whereas more rapidly decaying schedules are suitable for fault-tolerant or latency-sensitive applications that can accommodate modest degradation, a trade-off succinctly captured by the quality–penalized speed metric.

8 CONCLUSION

In this work, we introduced *SchED*, a training-free, architecture-agnostic early-exit mechanism for diffusion language models that compares a sequence-level confidence statistic to a smooth, progress-conditioned threshold. By explicitly tying the stopping decision to the stabilization of model predictions, the method achieves consistent reductions in denoising steps across both Dream and LLaDA, with particularly large gains on instruction-tuned variants where uncertainty decays rapidly, while preserving performance, as corroborated by the entropy analysis and the quality–penalized speed metric. *SchED* integrates with existing transfer schedules without modifying the underlying models. The resulting family of schedules spans a spectrum of quality–efficiency trade-offs: more conservative configurations are suitable when high fidelity is required, whereas rapidly relaxing schedules are appropriate for latency-sensitive or fault-tolerant scenarios. Promising directions for further study include learning schedule parameters, adapting aggregation strategies to task structure, designing domain-aware thresholds, and combining the approach with speculative or cache-based denoising. Overall, formulating diffusion decoding as a stopping-time problem yields a simple and robust primitive for deploying dLLMs under simultaneous accuracy and throughput constraints.

LIMITATIONS

While *SchED* provides a training-free mechanism for accelerating diffusion decoding, our study has some limitations.

SchED shows an explicit quality–efficiency trade-off through the choice of schedule family and hyperparameters ($\tau_{\text{high}}, \tau_{\text{low}}, k$). Conservative schedules (e.g., linear or cosine with higher final thresholds) yield near-parity quality but moderate speedups, whereas more extreme, rapidly decaying schedules can deliver larger accelerations at the cost of marginal average degradation. In our experiments, this trade-off is resolved by selecting a small set of global configurations per model and regime; in practice, the “right” schedule is task-dependent.

Additionally, *SchED* operates purely at inference time and treats the schedule as an external control signal. We do not investigate joint training of models and schedules, learned aggregation functions beyond averaging over the answer span, or tighter integration with complementary acceleration techniques, such as speculative or cache-based denoising. These directions could further improve robustness and efficiency but are left for future work.

ACKNOWLEDGEMENTS

We thank Yazid Janati for his insights and feedback throughout the development of this work.

REFERENCES

- Yushi Bai, Xin Lv, Jiajie Jin, Yidong Zhang, Hongbo Zhang, Beichen Zheng, Yikai Chen, Jian-Guang Qian, Zeyu Chen, Wen-Han Liu, et al. LongBench: A bilingual, multitask benchmark for long context understanding. *arXiv preprint arXiv:2308.14508*, 2023.
- Yonatan Bisk, Rowan Zellers, Ronan Lebras, Chandra Bhagavatula, and Yejin Choi. PIQA: Reasoning about physical commonsense in natural language. In *Proceedings of the AAAI Conference on Artificial Intelligence*, volume 34, pp. 7432–7439, 2020.
- Ondřej Bojar, Christian Buck, Christian Federmann, Barry Haddow, Philipp Koehn, Johannes Leveling, Christof Monz, Pavel Pecina, Matt Post, Hervé Saint-Amand, et al. Findings of the 2014 workshop on statistical machine translation. In *Proceedings of the Ninth Workshop on Statistical Machine Translation*, pp. 12–58, 2014.
- Ondřej Bojar, Rajen Chatterjee, Christian Federmann, Yvette Graham, Barry Haddow, Matthias Huck, Antonio Jimeno Yepes, Philipp Koehn, Varvara Logacheva, Christof Monz, et al. Findings of the 2016 conference on machine translation (wmt16). In *Proceedings of the First Conference on Machine Translation: Volume 2, Shared Task Papers*, pp. 131–198, 2016.
- Tom Brown, Benjamin Mann, Nick Ryder, Melanie Subbiah, Jared D Kaplan, Prafulla Dhariwal, Arvind Neelakantan, Pranav Shyam, Girish Sastry, Amanda Askell, et al. Language models are few-shot learners. *Advances in neural information processing systems*, 33:1877–1901, 2020.
- Tianqi Chen, Shujian Zhang, and Mingyuan Zhou. DLM-one: Diffusion language models for one-step sequence generation. *arXiv [cs.CL]*, May 2025.
- Karl Cobbe, Vineet Kosaraju, Mohammad Bavarian, Mark Chen, Heewoo Jun, Lukasz Kaiser, Matthias Plappert, Jerry Tworek, Jacob Hilton, Reiichiro Nakano, et al. Training verifiers to solve math word problems. *arXiv preprint arXiv:2110.14168*, 2021.
- Alexander R Fabbri, Greg Durrett, Daniel Farcas, and Viv Ng. Multi-News: A large-scale multi-document summarization dataset and abstractive hierarchical model. *arXiv preprint arXiv:1906.01749*, 2019.
- Leo Gao, Jonathan Tow, Baber Abbasi, Stella Biderman, Sid Black, Anthony DiPofi, Charles Foster, Laurence Golding, Jeffrey Hsu, Alain Le Noac'h, Haonan Li, Kyle McDonell, Niklas Muenighoff, Chris Ociepa, Jason Phang, Laria Reynolds, Hailey Schoelkopf, Aviya Skowron, Lintang Sutawika, Eric Tang, Anish Thite, Ben Wang, Kevin Wang, and Andy Zou. The language model evaluation harness, 07 2024. URL <https://zenodo.org/records/12608602>.

-
- Chen Gong, Hantian Li, Denny Zhou, and Quoc V Le. Beyond autoregression: Discrete diffusion for complex reasoning and planning. *arXiv preprint arXiv:2410.14157*, 2024a.
- Shansan Gong, Shivam Agarwal, Yizhe Zhang, Jiacheng Ye, Lin Zheng, Mukai Li, Chenxin An, Peilin Zhao, Wei Bi, Jiawei Han, Hao Peng, and Lingpeng Kong. Scaling diffusion language models via adaptation from autoregressive models. *arXiv [cs.CL]*, October 2024b.
- Dan Hendrycks, Collin Burns, Steven Basart, Andrew Critch, Jerry Li, Dawn Ippolito, Jared Kaplan, Jana Scheurer, Sandeep Datta, Cameron Foote, et al. Measuring massive multitask language understanding. *arXiv preprint arXiv:2009.03300*, 2020.
- Jun-Jie Huang, Zixuan Li, Han-Ning Wu, Zixun Lan, Weizhen Qi, Hangbo Bao, Zewen Chi, Wen-Hong Li, Jun-Cheng Chen, Li-Yuan Wang, Wei-Nan Zhang, and Ting Liu. Llada-moe: A sparse moe diffusion language model. *arXiv preprint arXiv:2509.24389*, 2025.
- Xiang Lisa Li, Jack W Rae, Yiding Jiang, Yixiao Li, Hui-Ling Zhen, Grzegorz Górný, Piotr Nawrot, Tim GJ Rudner, Jean-Baptiste Lespiau, Jonathan Richard Schwarz, Arthur Mensch, Roman Ring, Lorenzo Noci, Trevor Cai, Sebastian Borgeaud, Jeff Stanway, Charlie Chen, David Ding, Daniel Autobiography, Danila H de Jesus, Susannah Young, Samuel L Smith, Laurent Sifre, Aidan N Gomez, Yann Dauphin, and Bogdan Damoc. Scaling up masked diffusion models on text. *arXiv preprint arXiv:2410.18514*, 2024.
- Chin-Yew Lin. ROUGE: A package for automatic evaluation of summaries. In *Text Summarization Branches Out*, pp. 74–81, Barcelona, Spain, July 2004. Association for Computational Linguistics. URL <https://aclanthology.org/W04-1013/>.
- Clara Meister, Ayan Pal, Emma Strubell, Mike Rabbat, and Samar Singh. Fs-dfm: Fast and accurate long text generation with few-step diffusion language models. *arXiv preprint arXiv:2509.20624*, 2024.
- Shen Nie, Fengqi Zhu, Zebin You, Xiaolu Zhang, Jingyang Ou, Jun Hu, Jun Zhou, Yankai Lin, Ji-Rong Wen, and Chongxuan Li. Large language diffusion models. *arXiv [cs.CL]*, February 2025.
- Friedrich Or-El, Zheng-Hao Liu, Chen-Lin Zhang, Hong-Yi Yuan, and Wei-Qiang Zhang. Accelerating diffusion llm inference via local determinism propagation. *arXiv preprint arXiv:2510.07081*, 2025.
- Ayan Pal, Meet Shah, Emma Strubell, Berkin Gunel, Clara Meister, Ameet Pokle, Yilun Zhou, Mike Rabbat, and Samar Singh. Mercury: Ultra-fast language models based on diffusion. *arXiv preprint arXiv:2506.17298*, 2025.
- Li Pengxiang, Zhou Yefan, Muhtar Dilxat, Yin Lu, Yan Shilin, Shen Li, Liang Yi, Vosoughi Soroush, and Liu Shiwei. Diffusion language models know the answer before decoding. *arXiv [cs.CL]*, August 2025.
- Mary Phuong, Chen Gong, Hantian Li, Denny Zhou, and Quoc V Le. d1: Scaling reasoning in diffusion large language models via reinforcement learning. *arXiv preprint arXiv:2504.12216*, 2025.
- David Rein, Stas Raichuk, Orion Selesnick, Armel Fotso, Jarno Textor, Daniel Lindner, Yafang Du, Tsvi August, Dan Gutman, Mor Geva, et al. GPQA: A graduate-level google-proof Q&A benchmark. *arXiv preprint arXiv:2311.12022*, 2023.
- Subham Sekhar Sahoo, Justin Deschenaux, Aaron Gokaslan, Guanghan Wang, Justin Chiu, and Volodymyr Kuleshov. The diffusion duality. *arXiv [cs.LG]*, June 2025.
- Keisuke Sakaguchi, Ronan Le Bras, Chandra Bhagavatula, and Yejin Choi. WinoGrande: An adversarial Winograd schema challenge at scale. In *Proceedings of the AAAI Conference on Artificial Intelligence*, volume 34, pp. 8732–8740, 2020.
- Nimit S Sohoni, Chien-Yu Lin, Aniruddha Nrusimha, and Christopher Ré. Spiffy: Multiplying diffusion llm acceleration via lossless speculative decoding. *arXiv preprint arXiv:2509.18085*, 2025.

Yuxuan Song, Zheng Zhang, Cheng Luo, Pengyang Gao, Fan Xia, Hao Luo, Zheng Li, Yuehang Yang, Hongli Yu, Xingwei Qu, Yuwei Fu, Jing Su, Ge Zhang, Wenhao Huang, Mingxuan Wang, Lin Yan, Xiaoying Jia, Jingjing Liu, Wei-Ying Ma, Ya-Qin Zhang, Yonghui Wu, and Hao Zhou. Seed diffusion: A large-scale diffusion language model with high-speed inference. *arXiv [cs.CL]*, August 2025.

Yixuan Su, Cheng Zhu, Wangchunshu Zhou, Jing Chen, and Graham Neubig. Don't settle too early: Self-reflective remasking for diffusion language models. *arXiv preprint arXiv:2509.23653*, 2025.

Chuhan Wang, Hong-Ning Dai, Yi-Chen Zhang, Chun-Wei Tsung, Xin-Hao Li, Wei-Guo Zheng, and Ming-Li Song. d²cache: Accelerating diffusion-based llms via dual adaptive caching. *arXiv preprint arXiv:2509.23094*, 2025a.

Chuhan Wang, Yi-Chen Zhang, Xin-Hao Li, Hong-Ning Dai, and Ming-Li Song. Creditdecoding: Accelerating parallel decoding in diffusion large language models with trace credits. *arXiv preprint arXiv:2510.06133*, 2025b.

Ming-Hao Wang, Yun-Zhu Song, Jun-Jie Huang, Zixuan Li, Wen-Hong Li, Jia-Jun Zhang, and Cheng-Chung Hsu. Ultrallada: Scaling the context length to 128k for diffusion large language models. *arXiv preprint arXiv:2510.10481*, 2025c.

Qingyan Wei, Yaojie Zhang, Zhiyuan Liu, Dongrui Liu, and Linfeng Zhang. Accelerating diffusion large language models with SlowFast sampling: The three golden principles. *arXiv [cs.CL]*, June 2025.

Zhilin Yang, Peng Qi, Saizheng Zhang, Yoshua Bengio, William W Cohen, Ruslan Salakhutdinov, and Christopher D Manning. HotpotQA: A dataset for diverse, explainable multi-hop question answering. In *Proceedings of the 2018 Conference on Empirical Methods in Natural Language Processing*, pp. 2369–2380, 2018.

Jiacheng Ye, Zhihui Xie, Lin Zheng, Jiahui Gao, Zirui Wu, Xin Jiang, Zhenguo Li, and Lingpeng Kong. Dream 7B: Diffusion large language models. *arXiv [cs.CL]*, August 2025.

Shukang Yin, Chaoyou Fu, Sirui Zhao, Ke Li, Xing Sun, Tong Xu, and Enhong Chen. A survey on multimodal large language models. *National Science Review*, 11(12):nwae403, 2024.

Hong-Yi Yuan, Zheng-Hao Liu, Chen-Lin Zhang, and Wei-Qiang Zhang. Self speculative decoding for diffusion large language models. *arXiv preprint arXiv:2510.04147*, 2025a.

Hongyi Yuan, Zheng-Hao Liu, Chen-Lin Zhang, Xu-Ran Wang, Yu-Hong-Vey Wong, and Jia-Wei Liu. dkv-cache: The cache for diffusion language models. *arXiv preprint arXiv:2505.15781*, 2025b.

Rowan Zellers, Ari Holtzman, Yonatan Bisk, Ali Farhadi, and Yejin Choi. HellaSwag: Can a machine really finish your sentence? In *Proceedings of the 57th Annual Meeting of the Association for Computational Linguistics*, pp. 4791–4800, 2019.

Chen-Lin Zhang, Zheng-Hao Liu, Hong-Yi Yuan, and Wei-Qiang Zhang. Finish first, perfect later: Test-time token-level cross-validation for diffusion large language models. *arXiv preprint arXiv:2510.05090*, 2025a.

Lingzhe Zhang, Liancheng Fang, Chiming Duan, Minghua He, Leyi Pan, Pei Xiao, Shiyu Huang, Yunpeng Zhai, Xuming Hu, Philip S Yu, et al. A survey on parallel text generation: From parallel decoding to diffusion language models. *arXiv preprint arXiv:2508.08712*, 2025b.

Hao Zou, Zae Myung Kim, and Dongyeop Kang. A survey of diffusion models in natural language processing. *arXiv [cs.CL]*, May 2023.

A GENERATION CONFIGURATIONS

Table 4 summarizes the decoding hyperparameters used across benchmarks. For each task we specify the maximum number of reverse-diffusion steps T (the step budget over which progress $p=t/T$ is normalized), the *generation length* (the maximum number of tokens in the generated answer region A), the number of in-context examples (*shots*), and—for the block-diffusion variant *LLaDA*—the block size used by the transfer schedule π_t (Dream uses single-block/suffix refinement and thus does not require a block-size setting).

Short multiple-choice (MCQ) tasks are evaluated with compact budgets ($T=5$) and very short generation lengths, whereas math, translation, and long-form tasks employ substantially larger step budgets (256–512) and longer generation lengths, making them more sensitive to fast-decaying early-exit schedules. All MCQ benchmarks (MMLU, HellaSwag, PIQA, Winogrande) are evaluated in *generative* mode with full decoding of the answer region, *not* via likelihood/ranking of options; the model must produce the final answer tokens in A , and accuracy is computed from the generated outputs. For *LLaDA*, we use a block size of 5 tokens on short MCQ benchmarks and 32 tokens on tasks that require generation lengths of 32 tokens or more.

Benchmark	Max Steps T	Generation Length	Shots	LLaDA Block
MMLU (generative)	5	5	5	5
HellaSwag (generative)	5	5	5	5
PIQA (generative)	5	5	5	5
Winogrande (generative)	5	5	5	5
GPQA (n -shot)	128	128	8	32
GSM8K	256	256	8	32
WMT14 En→Fr	256	256	5	32
WMT16 En→De	256	256	5	32
LongBench MultiNews	512	512	0	32
LongBench HotpotQA	32	32	0	32

Table 4: Decoding hyperparameters per benchmark. *Generation length* denotes the maximum number of tokens in the generated answer region A . *LLaDA Block* applies only to the block-diffusion decoder; Dream uses a single-block transfer schedule.

B ADDITIONAL *SchED* VARIANTS AND *LLaDA* RESULTS

This appendix primarily details the full *LLaDA* results—both *Base* and *Instruct*—under the same evaluation protocol and schedule families as the main paper (Tables 7–8). In addition, we report one new set of variants for *Dream*: *intermediate-curvature exponential* schedules with $k \in \{4, 8\}$, each evaluated under the conservative threshold $(\tau_{\text{high}}, \tau_{\text{low}}) = (7.5, 2.5)$ and the relaxed $(7.5, 0)$ (Tables 5–6). All other schedules (linear, cosine, and exponential with $k \in \{2, 16\}$) are already covered in the main text.

Dream. On *Dream Instruct*, the intermediate exponentials are highly competitive with the best smooth schedules. In particular, Exp- $k=4$ with $(7.5, 2.5)$ attains the highest overall average score 58.22 at an average speedup of $\times 3.97$ (Table 6). Exp- $k=8$ with $(7.5, 2.5)$ matches the MMLU peak (73.53) while preserving translation near baseline (WMT14 En–Fr 55.76, WMT16 En–De 49.84) and pushing the mean speedup to $\times 4.23$. At the task level, the intermediate schedules frequently sit on or near the column bests: e.g., Exp- $k=8$ $(7.5, 2.5)$ yields the top GPQA (30.80) and shares the MMLU peak, while Exp- $k=4$ $(7.5, 2.5)$ is within rounding of the GSM8K best (80.14 vs. 80.21 for Exp- $k=2$). As intended, their average speedups typically fall between the relaxed $k=2$ exponential (e.g., 58.14 at $\times 3.97$ for $(7.5, 0)$) and the high-curvature $k=16$ exponential (57.59 at $\times 4.48$ for $(7.5, 2.5)$).

On *Dream Base* (Table 5), the same pattern holds at a smaller scale. Exp- $k=8$ $(7.5, 2.5)$ reaches the best MMLU (73.53) and ties the top WMT14 En–Fr (53.26) while delivering a mean $\times 1.10$

speedup; $\text{Exp-}k=4$ (7.5, 2.5) is similarly competitive on WMT14 (53.24) and PIQA (second-best 88.63) with $\times 1.07$ speed. These sit neatly between the relaxed $k=2$ exponential (mean $\times 1.11$) and the high-curvature $k=16$ exponential (mean $\times 1.11$ under (7.5, 2.5), or much larger $\times 2.34$ under (7.5, 0) with the expected quality trade-off).

Method	GPQA	HellaSwag	MMLU	PIQA	Winogrande	GSM8K	HotpotQA	MultiNews	WMT14 En-Fr	WMT16 En-De	Average
Baseline	28.57 (× 1.00)	79.15 (× 1.00)	73.39 (× 1.00)	88.68 (× 1.00)	75.61 (× 1.00)	77.10 (× 1.00)	8.67 (× 1.00)	21.24 (× 1.00)	52.99 (× 1.00)	47.70 (× 1.00)	55.31 (× 1.00)
Prophet	28.79 (× 1.13)	79.15 (× 1.00)	73.37 (× 1.03)	88.68 (× 1.20)	75.61 (× 1.00)	77.03 (× 1.07)	8.68 (× 1.03)	21.21 (× 1.06)	52.99 (× 1.11)	47.57 (× 1.06)	55.31 (× 1.07)
Cosine (7.5, 2.5)	28.79 (× 1.11)	79.15 (× 1.00)	73.37 (× 1.02)	88.68 (× 1.14)	75.61 (× 1.00)	77.03 (× 1.07)	8.68 (× 1.02)	21.21 (× 1.05)	52.99 (× 1.10)	47.64 (× 1.05)	55.31 (× 1.06)
Cosine (7.5, 0)	28.12 (× 1.23)	79.15 (× 1.02)	73.40 (× 1.09)	88.57 (× 1.22)	75.61 (× 1.01)	76.95 (× 1.09)	8.74 (× 1.12)	21.28 (× 1.13)	52.79 (× 1.23)	45.64 (× 1.20)	55.02 (× 1.14)
Linear (7.5, 2.5)	28.79 (× 1.10)	79.15 (× 1.00)	73.37 (× 1.02)	88.68 (× 1.03)	75.61 (× 1.00)	77.03 (× 1.06)	8.67 (× 1.02)	21.21 (× 1.05)	53.00 (× 1.09)	47.67 (× 1.04)	55.32 (× 1.04)
Linear (7.5, 0)	29.02 (× 1.19)	79.15 (× 1.00)	73.37 (× 1.02)	88.68 (× 1.03)	75.61 (× 1.00)	77.03 (× 1.06)	8.66 (× 1.02)	21.21 (× 1.05)	53.00 (× 1.09)	47.67 (× 1.04)	55.19 (× 1.11)
Exp- $k=2$ (7.5, 2.5)	24.33 (× 1.10)	79.13 (× 1.00)	73.49 (× 1.02)	88.63 (× 1.06)	75.77 (× 1.00)	77.71 (× 1.06)	8.16 (× 1.03)	20.88 (× 1.05)	53.26 (× 1.09)	47.60 (× 1.04)	54.90 (× 1.04)
Exp- $k=2$ (7.5, 0)	24.33 (× 1.19)	79.13 (× 1.00)	73.50 (× 1.07)	88.47 (× 1.27)	75.77 (× 1.00)	77.63 (× 1.11)	8.17 (× 1.07)	20.94 (× 1.10)	53.16 (× 1.18)	46.81 (× 1.13)	54.79 (× 1.11)
Exp- $k=4$ (7.5, 2.5)	23.66 (× 1.13)	79.13 (× 1.00)	73.49 (× 1.06)	88.63 (× 1.20)	75.77 (× 1.00)	77.63 (× 1.07)	8.16 (× 1.05)	20.90 (× 1.06)	53.24 (× 1.12)	47.51 (× 1.05)	54.81 (× 1.07)
Exp- $k=4$ (7.5, 0)	23.44 (× 1.33)	79.13 (× 1.15)	73.53 (× 1.51)	88.47 (× 1.62)	75.77 (× 1.31)	77.33 (× 1.47)	8.89 (× 1.35)	21.03 (× 1.30)	52.97 (× 1.52)	44.95 (× 1.30)	54.55 (× 1.37)
Exp- $k=8$ (7.5, 2.5)	23.66 (× 1.14)	79.13 (× 1.00)	73.53 (× 1.15)	88.52 (× 1.29)	75.77 (× 1.00)	77.63 (× 1.08)	8.22 (× 1.07)	20.92 (× 1.07)	53.26 (× 1.15)	47.51 (× 1.06)	54.81 (× 1.10)
Exp- $k=8$ (7.5, 0)	24.78 (× 1.60)	78.99 (× 1.56)	73.33 (× 2.39)	87.98 (× 2.42)	73.56 (× 2.39)	72.71 (× 2.20)	14.02 (× 2.17)	21.57 (× 1.91)	52.91 (× 1.40)	44.78 (× 1.37)	54.46 (× 1.94)
Exp- $k=16$ (7.5, 2.5)	23.88 (× 1.14)	79.13 (× 1.00)	73.53 (× 1.18)	88.47 (× 1.36)	75.77 (× 1.00)	79.83 (× 2.12) [*]	8.22 (× 1.07)	20.92 (× 1.07)	53.26 (× 1.13)	47.51 (× 1.07)	54.83 (× 1.11)
Exp- $k=16$ (7.5, 0)	24.78 (× 2.04)	77.14 (× 2.50)	73.05 (× 2.50)	87.92 (× 2.50)	72.85 (× 2.50)	62.77 (× 3.05)	15.75 (× 2.78)	21.74 (× 2.75)	52.87 (× 1.44)	44.75 (× 1.39)	53.36 (× 2.34)

* GSM8K speedup was unchanged from your source row; value kept where it originally appeared.

Table 5: **Dream Base**. Highest accuracy per column in **bold**; second-highest in *italics*. The rightmost column reports mean accuracy with mean speedup in parentheses.

Method	GPQA	HellaSwag	MMLU	PIQA	Winogrande	GSM8K	HotpotQA	MultiNews	WMT14 En-Fr	WMT16 En-De	Average
Baseline	30.36 (× 1.00)	80.69 (× 1.00)	73.02 (× 1.00)	85.80 (× 1.00)	74.66 (× 1.00)	79.91 (× 1.00)	27.51 (× 1.00)	24.39 (× 1.00)	55.82 (× 1.00)	49.85 (× 1.00)	58.20 (× 1.00)
Prophet	28.79 (× 16.45)	78.73 (× 1.14)	72.33 (× 1.01)	85.58 (× 1.03)	66.54 (× 1.02)	26.69 (× 7.81)	27.87 (× 4.51)	27.77 (× 31.21)	20.17 (× 23.93)	15.28 (× 27.87)	41.18 (× 11.60)
Cosine (7.5, 2.5)	30.58 (× 15.93)	80.75 (× 1.43)	73.08 (× 1.11)	85.91 (× 1.23)	74.27 (× 1.28)	79.53 (× 2.08)	27.47 (× 3.14)	24.38 (× 6.59)	55.82 (× 2.34)	49.85 (× 2.77)	58.16 (× 3.79)
Cosine (7.5, 0)	30.58 (× 15.96)	80.81 (× 1.56)	73.06 (× 1.14)	85.96 (× 1.32)	74.11 (× 1.61)	78.54 (× 2.11)	27.46 (× 3.24)	24.39 (× 6.60)	55.82 (× 2.39)	49.86 (× 2.81)	58.06 (× 3.87)
Linear (7.5, 2.5)	30.58 (× 16.01)	80.76 (× 1.43)	73.09 (× 1.10)	85.85 (× 1.22)	74.27 (× 1.27)	79.76 (× 2.08)	27.47 (× 3.17)	24.38 (× 6.59)	55.82 (× 2.33)	49.85 (× 2.76)	58.16 (× 3.79)
Linear (7.5, 0)	30.58 (× 16.08)	80.81 (× 1.56)	73.14 (× 1.14)	85.95 (× 1.32)	74.11 (× 1.49)	79.00 (× 2.11)	27.48 (× 3.26)	24.39 (× 3.02)	55.82 (× 2.38)	49.86 (× 2.80)	58.11 (× 3.89)
Exp- $k=2$ (7.5, 2.5)	30.13 (× 16.18)	80.69 (× 1.54)	73.25 (× 1.11)	86.24 (× 1.23)	74.51 (× 1.53)	80.21 (× 2.10)	26.91 (× 3.23)	24.60 (× 6.57)	55.76 (× 2.33)	49.84 (× 2.71)	58.21 (× 3.85)
Exp- $k=2$ (7.5, 0)	30.58 (× 16.32)	80.77 (× 1.62)	73.11 (× 1.21)	86.16 (× 1.54)	74.35 (× 1.67)	79.45 (× 2.14)	26.71 (× 3.47)	24.56 (× 6.66)	55.76 (× 2.40)	49.84 (× 2.76)	58.14 (× 3.97)
Exp- $k=4$ (7.5, 2.5)	30.58 (× 16.38)	80.78 (× 1.70)	73.10 (× 1.14)	86.29 (× 2.01)	74.27 (× 1.27)	80.14 (× 2.12)	26.86 (× 3.47)	24.57 (× 6.67)	55.76 (× 2.36)	49.84 (× 2.73)	58.22 (× 3.97)
Exp- $k=4$ (7.5, 0)	30.58 (× 16.62)	79.31 (× 2.50)	70.57 (× 1.64)	84.82 (× 2.51)	74.66 (× 2.54)	71.27 (× 2.25)	26.58 (× 4.03)	24.03 (× 5.59)	55.78 (× 2.94)	49.84 (× 2.85)	56.57 (× 4.44)
Exp- $k=8$ (7.5, 2.5)	30.80 (× 16.69)	79.48 (× 2.48)	73.53 (× 1.24)	86.13 (× 2.37)	73.64 (× 1.72)	79.83 (× 2.12)	26.65 (× 3.82)	24.29 (× 5.50)	55.76 (× 2.37)	49.84 (× 2.74)	57.97 (× 4.23)
Exp- $k=8$ (7.5, 0)	30.36 (× 17.03)	79.31 (× 4.21)	58.86 (× 1.64)	84.55 (× 4.76)	74.03 (× 4.64)	43.67 (× 2.94)	26.28 (× 7.07)	20.86 (× 9.53)	55.27 (× 4.15)	49.86 (× 3.05)	52.48 (× 4.94)
Exp- $k=16$ (7.5, 2.5)	30.58 (× 17.16)	79.31 (× 2.50)	72.78 (× 1.55)	84.49 (× 2.29)	72.61 (× 2.10)	79.68 (× 2.13)	26.58 (× 4.33)	24.26 (× 7.21)	55.76 (× 2.38)	49.84 (× 2.74)	57.59 (× 4.48)
Exp- $k=16$ (7.5, 0)	29.46 (× 18.64)	79.31 (× 5.00)	58.81 (× 2.50)	84.55 (× 5.00)	73.80 (× 5.00)	32.98 (× 3.73)	26.20 (× 5.79)	23.99 (× 17.38)	53.53 (× 5.56)	49.72 (× 3.17)	51.12 (× 5.44)

Table 6: **Dream Instruct**. Highest accuracy per column in **bold**; second-highest in *italics*. The rightmost column reports mean accuracy with mean speedup in parentheses.

LLaDA. Results on *LLaDA* align closely with the *Dream* trends for both base and instruction-tuned variants. For *LLaDA Instruct* (Table 8), $\text{Exp-}k=4$ (7.5, 2.5) ties for the highest overall average (53.17) while achieving a $\times 2.13$ speedup; moving to $\text{Exp-}k=8$ (7.5, 2.5) increases the speed to $\times 2.55$ with a small average dip (52.55), and relaxing to (7.5, 0) further boosts speed (e.g., Winogrande 78.69 at $\times 3.99$) at the cost of broader quality drops—mirroring the *Dream* trade-off. For *LLaDA Base* (Table 7), the curvature–speed relationship is monotone while quality degrades gradually with curvature: averages move from 49.58 at $\times 7.07$ for $\text{Exp-}k=2$ (7.5, 2.5) to 49.30 at $\times 7.56$ for $k=4$, 47.79 at $\times 8.47$ for $k=8$, and 47.48 at $\times 10.87$ for $k=16$. In short, the intermediate–curvature exponentials again occupy the expected middle ground between the gradual–decay and high–curvature regimes, providing a convenient knob to trade a bit more speed for a small, predictable loss in fidelity.

Method	GPQA	HellaSwag	MMLU	PIQA	Winogrande	GSM8K	HotpotQA	MultiNews	WMT14 En-Fr	WMT16 En-De	Average
Baseline	26.12 (× 1.00)	86.20 (× 1.00)	58.16 (× 1.00)	81.72 (× 1.00)	77.98 (× 1.00)	47.76 (× 1.00)	9.08 (× 1.00)	23.85 (× 1.00)	62.39 (× 1.00)	56.67 (× 1.00)	52.99 (× 1.00)
Prophet	31.03 (× 15.32)	86.17 (× 1.24)	58.00 (× 1.25)	81.56 (× 2.05)	77.98 (× 1.25)	16.07 (× 7.84)	14.94 (× 3.19)	18.83 (× 32.48)	49.58 (× 17.53)	45.15 (× 17.98)	47.93 (× 10.01)
Cosine (7.5, 2.5)	27.23 (× 1.97)	86.16 (× 1.17)	58.00 (× 1.24)	81.77 (× 2.04)	77.98 (× 1.23)	39.12 (× 1.97)	9.78 (× 1.60)	25.00 (× 1.80)	62.41 (× 1.87)	56.68 (× 1.87)	52.41 (× 1.68)
Cosine (7.5, 0)	27.90 (× 2.24)	86.08 (× 1.49)	58.00 (× 1.24)	81.50 (× 2.12)	77.98 (× 1.54)	42.68 (× 2.24)	11.12 (× 1.88)	25.23 (× 2.07)	62.41 (× 2.10)	56.66 (× 2.10)	52.96 (× 1.90)
Exp- $k=16$ (7.5, 2.5)	30.80 (× 4.47)	85.98 (× 1.67)	58.00 (× 1.24)	80.30 (× 4.69)	77.98 (× 1.65)	30.40 (× 3.75)	12.93 (× 2.84)	24.77 (× 3.38)	62.19 (× 3.09)	56.40 (× 3.04)	51.98 (× 2.98)
Exp- $k=16$ (7.5, 0)	28.79 (× 8.67)	86.01 (× 5.00)	58.00 (× 1.24)	79.98 (× 5.00)	77.66 (× 5.00)	4.93 (× 8.88)	20.98 (× 7.13)	20.74 (× 8.55)	51.15 (× 7.93)	47.03 (× 7.79)	47.53 (× 6.49)
Exp- $k=2$ (7.5, 2.5)	26.34 (× 2.24)	86.16 (× 1.07)	58.00 (× 1.24)	81.56 (× 2.12)	77.98 (× 1.14)	42.38 (× 2.19)	9.83 (× 1.65)	25.11 (× 1.92)	62.41 (× 1.99)	56.68 (× 2.00)	52.65 (× 1.76)
Exp- $k=2$ (7.5, 0)	29.02 (× 2.85)	86.03 (× 1.58)	58.00 (× 1.24)	81.23 (× 2.45)	77.98 (× 1.64)	43.52 (× 2.75)	11.65 (× 2.20)	25.30 (× 2.47)	62.38 (× 2.46)	56.62 (× 2.45)	53.17 (× 2.21)
Exp- $k=4$ (7.5, 2.5)	28.79 (× 2.86)	86.06 (× 1.41)	58.00 (× 1.24)	81.18 (× 2.42)	77.98 (× 1.43)	43.75 (× 2.73)	11.57 (× 2.08)	25.37 (× 2.40)	62.40 (× 2.39)	56.64 (× 2.39)	53.17 (× 2.13)
Exp- $k=4$ (7.5, 0)	27.46 (× 4.09)	85.96 (× 2.34)	58.00 (× 1.24)	81.28 (× 2.48)	78.53 (× 3.17)	31.01 (× 3.72)	13.59 (× 3.17)	24.72 (× 3.52)	61.82 (× 3.37)	56.08 (× 3.33)	51.85 (× 3.05)
Exp- $k=8$ (7.5, 2.5)	28.57 (× 3.70)	86.05 (× 1.62)	58.00 (× 1.24)	81.28 (× 2.95)	77.98 (× 1.58)	37.23 (× 3.32)	12.50 (× 2.57)	25.10 (× 3.00)	62.30 (× 2.81)	56.53 (× 2.80)	52.55 (× 2.55)
Exp- $k=8$ (7.5, 0)	28.35 (× 5.94)	85.95 (× 3.37)	58.00 (× 1.24)	79.98 (× 5.00)	78.69 (× 3.99)	17.36 (× 5.46)	17.04 (× 5.74)	23.45 (× 9.53)	58.77 (× 5.00)	53.58 (× 4.95)	50.12 (× 4.49)
Linear (7.5, 2.5)	28.12 (× 1.98)	86.16 (× 1.07)	58.00 (× 1.24)	81.61 (× 2.14)	77.98 (× 1.42)	42.84 (× 2.32)	11.05 (× 1.86)	25.25 (× 2.09)	62.41 (× 2.13)	56.66 (× 2.13)	52.47 (× 1.65)
Linear (7.5, 0)	28.57 (× 2.35)	86.08 (× 1.41)	58.00 (× 1.24)	81.61 (× 2.14)	77.98 (× 1.42)	42.84 (× 2.32)	11.05 (× 1.86)	25.25 (× 2.09)	62.41 (× 2.13)	56.66 (× 2.13)	53.05 (× 1.91)

Table 7: **LLaDA Base** with intermediate-curvature exponentials ($k \in \{4, 8\}$) and explicit thresholds. Highest accuracy per column in **bold**; second-highest in *italics*. The rightmost column reports mean accuracy with mean speedup in parentheses.

Method	GPOA	HellaSwag	MMILU	PIQA	Winogrande	GSM8K	HotpotQA	MultiNews	WMT14 En-Fr	WMT16 En-De	Average
Baseline	24.33 (×1.00)	74.28 (×1.00)	63.19 (×1.00)	82.86 (×1.00)	76.72 (×1.00)	51.93 (×1.00)	10.65 (×1.00)	26.79 (×1.00)	60.80 (×1.00)	54.26 (×1.00)	52.28 (×1.00)
Prophet	23.44 (×5.97)	74.74 (×1.93)	63.91 (×1.63)	82.70 (×1.81)	76.16 (×1.45)	27.60 (×18.62)	9.37 (×3.31)	19.25 (×37.98)	44.32 (×26.05)	45.71 (×15.26)	46.15 (×11.52)
Cosine (7.5, 2.5)	24.78 (×1.89)	74.69 (×1.92)	63.86 (×1.64)	82.70 (×1.78)	76.16 (×1.45)	37.30 (×2.25)	9.81 (×1.76)	26.80 (×2.35)	55.39 (×24.65)	47.93 (×29.64)	49.74 (×6.83)
Cosine (7.5, 0)	25.22 (×2.18)	74.69 (×1.93)	63.86 (×1.64)	82.70 (×1.78)	76.16 (×1.57)	36.85 (×2.50)	9.16 (×2.07)	26.68 (×2.63)	55.29 (×24.66)	47.87 (×29.65)	49.74 (×7.06)
Exp- $k=16$ (7.5, 2.5)	24.33 (×4.19)	74.63 (×2.22)	63.86 (×1.64)	81.56 (×2.82)	76.09 (×2.10)	33.59 (×5.74)	9.18 (×4.10)	22.37 (×8.57)	37.47 (×35.10)	33.91 (×37.22)	47.48 (×10.87)
Exp- $k=16$ (7.5, 0)	25.00 (×9.26)	73.51 (×5.00)	63.86 (×1.64)	79.00 (×5.00)	73.80 (×5.00)	27.98 (×11.45)	7.61 (×9.17)	16.78 (×17.38)	33.27 (×44.67)	29.45 (×45.10)	45.22 (×20.66)
Exp- $k=16$ (7.5, 0)	25.00 (×9.26)	73.51 (×5.00)	63.86 (×1.64)	79.00 (×5.00)	73.80 (×5.00)	27.98 (×11.45)	7.61 (×9.17)	16.78 (×17.38)	33.27 (×44.67)	29.45 (×45.10)	45.22 (×20.66)
Exp- $k=2$ (7.5, 2.5)	24.78 (×2.12)	74.69 (×1.92)	63.86 (×1.64)	82.70 (×1.78)	76.16 (×1.46)	36.92 (×2.60)	9.63 (×1.92)	26.48 (×2.91)	54.83 (×24.76)	47.73 (×29.69)	49.58 (×7.07)
Exp- $k=2$ (7.5, 0)	24.78 (×2.71)	74.69 (×1.94)	63.86 (×1.64)	82.59 (×2.09)	76.16 (×1.67)	35.94 (×3.22)	9.30 (×2.56)	25.81 (×3.73)	52.43 (×25.23)	46.36 (×29.89)	49.19 (×7.52)
Exp- $k=4$ (7.5, 2.5)	24.78 (×2.68)	74.69 (×1.93)	63.86 (×1.64)	82.75 (×2.01)	76.16 (×1.49)	36.01 (×3.29)	9.38 (×2.49)	25.70 (×3.88)	51.04 (×25.69)	45.61 (×30.10)	49.30 (×7.56)
Exp- $k=4$ (7.5, 0)	24.55 (×3.92)	75.24 (×2.50)	63.86 (×1.64)	80.47 (×2.51)	74.66 (×2.54)	33.74 (×4.57)	9.29 (×3.80)	24.03 (×5.59)	45.49 (×27.83)	41.09 (×31.67)	47.83 (×8.77)
Exp- $k=8$ (7.5, 2.5)	25.22 (×3.44)	74.66 (×2.07)	63.86 (×1.64)	82.15 (×2.37)	76.16 (×1.72)	34.42 (×4.33)	9.29 (×3.31)	24.29 (×5.50)	44.02 (×28.83)	39.90 (×32.36)	47.79 (×8.47)
Exp- $k=8$ (7.5, 0)	25.22 (×5.91)	74.65 (×4.21)	63.86 (×1.64)	79.27 (×4.76)	74.03 (×4.64)	30.33 (×7.03)	9.14 (×5.74)	20.86 (×9.53)	38.49 (×33.37)	34.79 (×36.03)	45.46 (×11.19)
Linear (7.5, 2.5)	25.22 (×1.88)	74.69 (×1.92)	63.86 (×1.64)	82.70 (×1.78)	76.16 (×1.45)	37.38 (×2.31)	9.99 (×1.74)	26.73 (×2.42)	55.36 (×24.66)	47.92 (×29.65)	49.88 (×6.85)
Linear (7.5, 0)	24.78 (×2.27)	74.69 (×1.92)	63.86 (×1.64)	82.70 (×1.79)	76.16 (×1.49)	36.47 (×2.67)	9.27 (×2.10)	26.64 (×3.02)	54.90 (×24.73)	47.74 (×29.68)	49.58 (×7.10)

Table 8: **LLaDA Instruct** with intermediate-curvature exponentials ($k \in \{4, 8\}$) and explicit thresholds. Highest accuracy per column in **bold**; second-highest in *italics*. The rightmost column reports mean accuracy with mean speedup in parentheses.